ACS APPLIED MATERIALS & INTERFACES

Research Article

www.acsami.org

Thermoresponsive Cellulosic Hydrogels with Cell-Releasing Behavior

Siew P. Hoo,[†,‡] Fatemeh Sarvi,[§] Wai Ho Li,[∥] Peggy P.Y. Chan,[*,‡,⊥] and Zhilian Yue[*,‡,#]

[†]Department of Chemical Engineering, Monash University, Australia

[‡]MicroNanophysics Research Laboratory, School of Applied Science, RMIT University, Australia

[§]Department of Mechanical and Aerospace Engineering, Monash University, Australia

[∥]Monash Vision group, Monash University, Australia

[⊥]Melbourne Centre for Nanofabrication, Clayton, Australia

[#]ARC Centre of Excellence for Electromaterials Science, Intelligent Polymer Research Institute, University of Wollongong, Australia

ABSTRACT: Here we report the preparation and characterization of thermoresponsive cellulosic hydrogels with cell-releasing behavior. Hydroxypropyl cellulose (HPC) was modified with methacrylic anhydride (MA). The resultant macromonomer, HPC-MA, retains the characteristic thermoresponsive phase behavior of HPC, with an onset temperature of 36 °C and a lower critical solution temperature (LCST) of 37−38 °C, as determined by turbidity measurement. Homogenous HPC-MA hydrogels were prepared by UV-cross-linking the aqueous solutions of the macromonomer at room temperature, and characterized by water contact angle and swelling ratio measurements, and dynamic mechanical analysis. These hydrogels exhibit temperature-dependent surface hydrophilicity and hydrophobicity, equilibrium water content as well as mechanical properties. Cell-releasing characteristics were demonstrated using African green monkey kidney cell line (COS-7 cells) and murine-derived embryonic stem cell line (Oct4b2). By reducing temperature to 4 °C, the cultivated cells spontaneously detached from the hydrogels without the need of trypsin treatment. These unique properties make our HPC-MA hydrogels potential substrates for cell sheet engineering.

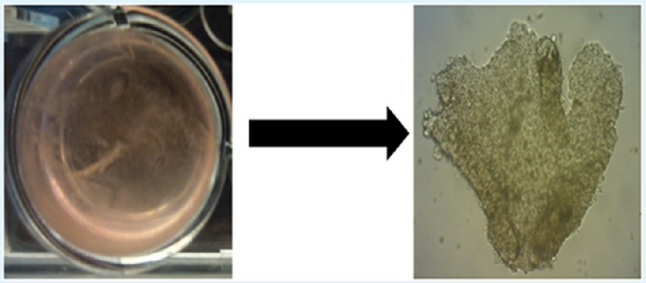

KEYWORDS: *thermoresponsive hydrogels, cellulose, lower critical solution temperature, murine-derived embryonic stem cells, cell sheet engineering*

INTRODUCTION

There has been extensive research into intelligent substrates that allow for spontaneous cell harvesting in response to an environmental stimulus.[1−3] A typical example is the thermoresponsive culture dishes prepared by grafting nanometer-sized poly(*N*-isopropylacrylamide) (PNIPAAm), or its copolymers, onto commercial tissue culture polystyrene dishes.[4] PNIPAAm undergoes a distinct phase transition from a dehydrated, collapsed structure to a highly hydrated, extended structure across a lower critical solution temperature (LCST) of 32 °C.[5,6] Such thermosensitive nature allows controlled alteration of surface hydrophobicity and hydrophilicity of the PNIPAAm-grafted dishes and, consequently, cell adhesion and detachment, by a small change in temperature. When temperature is below the LCST, cells cultivated on the substrate spontaneously detach as intact cell sheets with retained cell-to-cell junctions and extracellular matrix proteins, without the use of traditional methods involving enzymatic digestion or mechanical treatment.[7,8] Cell sheet engineering represents a novel scaffold-free approach suited for the regeneration of cell-dense tissues such as skin,[9] corneal,[10] cardiac,[11,12] esophageal, and hepatic[13] tissues.

Efforts have been made into extending the thermoresponsive culture surfaces with thermoresponsive hydrogels for cell sheet engineering. The highly hydrated structures and soft-tissue-like biomechanical properties of hydrogels and, more importantly, their capability for sustained delivery of bioactive molecules can provide a more physiologically relevant environment for the cultivated cells. For example, interpenetrating nanocomposite hydrogels have been prepared from hectorite clay nanoparticles, PNIPAAm and alginate. The presence of alginate has shown to significantly accelerate cell detachment, as a result of improved water penetration in the resulting hydrogels.[14] Although NIPAAm have been demonstrated to be a promising substrate for cell sheet engineering, NIPAAm is not derived from renewable resources, and NIPAAm does induce cellular cytotoxicity at physiological temperature.[15]

A number of studies have attempted to developed new thermoresponsive substrates to engineer cell sheets. For example, hydroxybutyl chitosan,[16] poly(*N*-isopropylacrylamide)/clay nanocomposite hydrogel,[17] methylcellulose/collagen hydrogel,[18] poly(*N*-isopropylacrylamide-*co*-acrylic acid)-*b*-poly(L-lactic acid),[19] and elastic protein-based polymer.[20] Some studies have attempted to engineer cell sheets using non-

Received: March 13, 2013
Accepted: June 4, 2013
Published: June 4, 2013

   dx.doi.org/10.1021/am4009133 | *ACS Appl. Mater. Interfaces* 2013, 5, 5592−5600

thermoresponsive substrate; for example, Guillaume-Gentil et al.[21] developed a RGD-modified poly(L-lysine)-*graft*-poly(ethylene glycol) substrate that can release cell sheet upon electrochemical polarization; Edahiro et al.[22] developed a photoresponsive NIPAAm-nitrospiropyran substrate that releases cells after UV irradiation and low temperature washing; Nagai et al.[23] developed a salmon atelocollagen fibrillar gel that releases cell sheet when subjected to collagenase digestion. Table 1 listed the substrates that have been studied for cell sheet engineering.

Table 1. Summary of Different Substrates Used for Cell Sheet Engineering

substrate material	release mechanism	ref
poly(*N*-isopropylacrylamide) (PIPAAm)	thermoresponsive	48
hydroxybutyl chitosan	thermoresponsive	16
poly(*N*-isopropylacrylamide)/clay nanocomposite hydrogel	thermoresponsive	17
methylcellulose/PBS/collagen hydrogel	thermoresponsive	18
elastic protein based polymer	thermoresponsive	20
poly(*N*-isopropylacrylamide-*co*-acrylic acid)-*b*-poly(L-lactic acid)	thermoresponsive	19
RGD-modified poly(L-lysine)-*graft*-poly(ethylene glycol)	electrochemical polarization	21
poly(*N*-isopropylacrylamide)-nitrospiropyran	photoresponsive	22
salmon atelocollagen fibrillar gel	collagenase digestion	23

Due to the many promising applications of thermoresponsive polymer, new thermoresponsive polymer systems with new biochemical properties, new physiochemical properties, lower cytotoxicities, and preferably derived from renewable resources, are still needed to provide multifunctional platforms. Herein, we report the preparation of a thermoresponsive hydrogel based on hydroxypropyl cellulose (HPC). HPC is a commercial derivative of cellulose, the most abundant renewable polysaccharide resource; it shows no cytotoxicity and has been approved by the Food and Drug Administration (FDA) as an agent for drug delivery applications. Also, HPC is soluble in water and many organic solvents. This has partly contributed to its use in biomedical and pharmaceutical applications. More importantly, for this study, HPC exhibits a phase transition from isotropic aqueous solution to metastable biphasic system above its LCST.[24−28] In this work, HPC was modified with bifunctional methacrylic anhydride (MA). The resulting polymer contains photocross-linkable methacrylate pendant group, namely HPC-MA. The thermoresponsive properties such as turbidity, water contact angle, swelling ratio, and dynamic mechanical analysis of these HPC-MA hydrogel were evaluated. Temperature-modulated cell-releasing characteristics were studied using COS-7 (African green monkey kidney) cell line and Oct4b2 (murine-derived embryonic stem cell) cell line.

MATERIALS AND METHODS

Synthesis. All chemicals used were purchased from Sigma-Aldrich, Australia, unless otherwise stated. Hydroxypropyl cellulose (HPC, M_n = 10 000 g/mol, degree of etherification ∼ 3.4, as determined previously by ^{1}H NMR[24]) was dehydrated by azeotropic distillation in toluene. The HPC hydrogel precursor was prepared by modifying HPC with methacrylic anhydride (MA). Briefly, the dehydrated HPC (4.0 g) was dissolved in chloroform (150 mL). MA (4.17 mmol) followed by *N*,*N*-dicyclohexylcardodiimide (DCC, 4.17 mmol) was added dropwise in chloroform, respectively. The solution was then stirred for 48 h in the presence of 4-dimethylaminopyrinde (DMAP, 0.4 g) as catalyst. The solution was concentrated and precipitated into diethyl ether. The polymer was then collected, redissolved in chloroform and precipitated into diethyl ether. Finally, the product was dissolved in water, filtered to remove any insoluble impurities, and dialyzed against deionized water for 72 h before lyophilization in a freeze-dryer (HETO PowerDry PL6000, Thermo Scientific, Australia). It was denoted as HPC-MA and characterized by ^{1}H NMR spectroscopy in $CDCl_3$. ^{1}H NMR ($CDCl_3$, δppm): 0.5−1.5 ($-CH_3-CH-$), 1.8−2.0 ($CH_3-C=CH_2$), 5.5−6.2 ($-C=CH_2$), 2.5−5.3 (other protons). The degree of modification of HPC-MA is defined as the number of MA groups per repeating unit, and determined by ^{1}H NMR spectroscopy.

Turbidimetry Measurement of HPC-MA in Deionized Water. The turbidity of HPC-MA was investigated by dissolving the lyophilize HPC-MA in deionized water to form a 15% (w/v) aqueous solution. The transmittance of the sample was monitored as a function of temperature at a fixed wavelength of 500 nm, using a UV−vis spectrophotometer (Agilent Technologies Cary 60 UVVIS, Australia) with the sample cell temperature controlled with a circulating water bath. The onset temperature was defined as the temperature at which signs of opaqueness were first observed. The transmittance was measured four times and the average value of the measurement was taken.

Preparation of HPC-MA Hydrogels. HPC-MA was dissolved in deionized water at 15% or 20% (w/v), to which a photoinitiator 2-hydroxy-1-[4-(2-hydroxyethoxy)phenyl]-2-methyl-1-propanone was added to a concentration of 4% (w/w) of the polymer weight, equivalent to a final concentration of 0.6% for HPC-MA-15% and 0.8% (w/v) for HPC-MA-20%. The solution was first warmed to 40−45 °C to allow the photonitiator to dissolve, the solution was then allowed to cool down to room temperature before cross-linking. The solution was cross-linked with UV light (320−405 nm, 200 mW cm^{-2}) at a distance of approximately 200 mm using an UV cross-linker (Honle UV Technology, UV-F 400, Germany) for approximately 6 min. The cross-linked gels were then washed with deionized water to remove any uncross-linked HPC-MA and the photoinitiator to minimize possible cytotoxicity effect from residual photoinitiator. The hydrogel prepared from 15% and 20% (w/v) of HPC-MA are denoted as HPC-MA-15% and HPC-MA-20%, respectively.

Water Contact Angle Measurement. Static contact angles were measured using the static sessile drop method by employing water contact angle equipment (OCA 20, DataPhysics Instrument, GmbH, Germany) equipped with automatic dispenser. In this experiment, a 10 μL deionized water droplet was dropped on the surface of the gel and the angle is measured by using the circle fit. To examine the dependence of contact angle on temperature, 25, 37, and 42 °C were selected as the testing temperatures.

Equilibrium Swelling Measurement. The as-prepared hydrogels were submerged in water at 4, 25, 37, and 42 °C for 48 h. The weight of the swollen sample (W_h) was measured after wiping off the excess water with a piece of filter paper. The weight of the dried sample (W_d) was measured after drying the swollen sample in an vacuum oven at 40 °C for 48 h. The weight of samples dehydrated using vacuum oven at 40 °C for 48 h were compared to the weight of samples prepared with the same formulation but dehydrated by lyophilization for 5 days; no significant weight difference was noted. The swelling ratio, SR, of the hydrogel was calculated according to eq 1. Each sample was measured three times from the four parallel specimens, and the average value of the measurement was taken.

$$\mathrm{SR} = \frac{W_h - W_d}{W_d} \quad (1)$$

Dynamic Mechanical Analysis. The storage moduli of HPC-MA-15% and HPC-MA-20% were tested on a dynamic mechanical analyzer (DMA) add in software (TA Instruments, Q800) at a frequency of 1 Hz and a preload of 0.01 N over a temperature range of 25−45 °C under compression mode. The testing was performed under atmospheric condition with a heating rate of 1 °C min^{-1}.

Cell Culture. All culture mediums used were obtained from Gibco, Australia, unless stated otherwise. The Oct4b2 cell lines that possess a

Scheme 1. Synthesis Scheme of HPC-MA

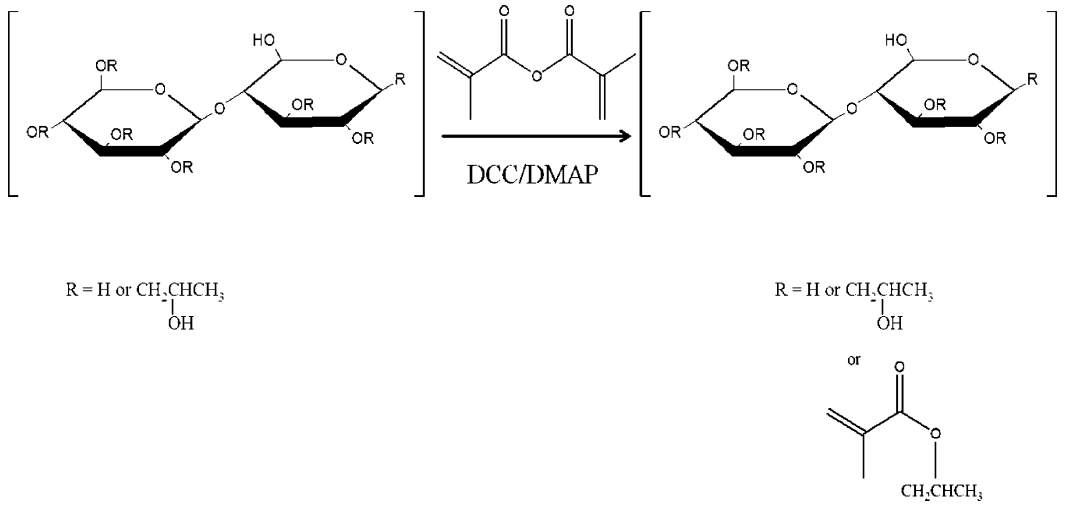

green fluorescent protein (GFP) under the control of the Oct4 promoter (Oct4-GFP)[29] were cultured according to the procedure reported in Sarvi et al.[30] Prior to cell seeding, Oct4b2 cells were cultured on 0.1% gelatin-coated dish with knockout medium supplemented with 20% knockout serum replacement, 1% nonessential amino acids, 0.1 mM 2-mercaptoethanol, 2 mM Glutamax, 1% penicillin-streptomycin (P/S), and 1000 U/mL murine leukemia inhibitory factor (mLIF, Chemicon, Australia). COS-7 cells were grown and maintained in Dulbecco's modified Eagle's medium (DMEM) supplemented with 10% fetal bovine serum (FBS), 2 mM L-glutamine, and 50 units/mL penicillin-streptomycin (P/S). Both COS-7 and Oct4b2 cells were cultured in a 37 °C, humidified 5% CO_2 incubator.

Temperature-Dependent Cell Release. HPC-MA-20% scaffolds with dimensions of 1.6 cm diameter by 0.5 cm thickness were sterilized by soaking in 70% ethanol overnight followed by washing with sterile phosphate buffered saline (PBS) before cell seeding. COS-7 and Oct4b2 cells were seeded with a cell density of 2×10^4 cells per scaffold. 10% (v/v) of gelatin was added to the culture media to improve cell adhesion. The plate was incubated at 37 °C in a humidified 5% CO_2 incubator for 3 h for cell attachment, and then 1 mL of fresh culture medium was added and the cells were allowed to cultivate on the hydrogel. COS-7 and Oct4b2 cells detachment was carried out at selected time point by incubating the culture plates at 4 °C for 30 and 10 min, respectively. Culture medium containing the detached cells was transferred to a new well-plate for reculturing to determine the regrowth ability of the retrieved cells. Images of cells at each stage of the process were visualized using fluorescent microscopy (Nikon, Eclipse Ti).

Cell Proliferation Assay. The viability of the recultured COS-7 cells was analyzed using the alamarBlue assay on days 1 to day 4. At each time point, 200 μL of 10% alamarBlue dye (diluted with complete medium) was added to each well containing cold treated cells and each well containing control cells (cells cultured on well-plate without cold treatment). The well-plate was then incubated at 37 °C for 4 h in a humidified 5% CO_2 incubator. Fluorescence analysis using an excitation wavelength of 570 nm and emission wavelength of 600 nm was carried out with a microplate reader (SynergyTM Mx, Biotek). The viability of cells was expressed as the percentage of alamarBlue reduction. Cells that have not been cultured on hydrogel and have not subjected to cold treatment were cultured on a well-plate and used as control.

The number of cells proliferating on the hydrogel was determined by quantifying the DNA content using PicoGreen assay kit (Quanti-iT PicoGreen dsDNA Reagent, Life Technologies, Australia) according to the manufacturer protocol. In brief, the cells were trypsinized from substrate and centrifuge for 5 min at 1200 rpm. The cell pellet was rinsed by cold PBS twice each followed by centrifugation for 5 min at 1200 rpm. The resultant cell pellet was collected by discarding the supernatant. The cells were lysed using 100 μL of NP40 cell lysis buffer (Life Technologies, Australia) for 30 min on ice and vortexed at 10 min intervals. The extract was transferred to microcentrifuge tubes and centrifuge at 13 000 rpm for 10 min at 4 °C. The clear lysate was aliquoted to clean microcentrifuge tube where 100 μL of PicoGreen reagent was added and allowed to incubate for 5 min at room temperature in the dark. The final solution was transferred into a 96-well plate, and the fluorescence was read using a microplate reader at excitation wavelength 480 nm and emission wavelength 520 nm. The number of cells in the sample was determined by correlating the DNA content with a DNA standard curve. The DNA standard curve was determined using cell lysates with known number of cells. In a separate experiment, the COS-7 cells were cultured on hydrogel followed by cold treatment on day 4, the harvested cells were readhered on culture dish and allowed to proliferate for 5 days. To examine the proliferation of the cold treated cells, COS-7 cells were first cultured on the hydrogels for 4 days followed by 4 °C cold treatment, the harvested cells were transferred to culture dish without further trypsinization, these cells were allowed to culture for another 5 days, and the DNA contents were quantified using the PicoGreen assay as described above.

Statistical Analysis. All experiments were performed in at least three replicates. Results were reported as average value ± standard deviation. One-way analysis of variance (ANOVA) was used to compare multiple groups of data statically; p values lower than 0.05 were considered statistically significant.

RESULTS AND DISCUSSION

Preparation of HPC-MA Macromonomer. HPC-MA was synthesized using a scheme illustrated in Scheme 1. DCC has been used for activation of carboxylic acids for coupling of cellulose derivatives with DMAP as catalyst.[31,32] DCC is known as a condensation reagent for producing anhydrides from corresponding acids with the formation of urea byproduct. The limitation of using anhydride is that only half the acid is stoichiometrically coupled and the other half is wasted[33] (i.e., released in the form of less reactive acid form). The use of DCC here is to react with these acids to regenerate anhydrides therefore improving the reaction efficacy. The degree of substitution (DS) was determined to be ~0.4 by ^{1}H NMR spectroscopy. HPC-MA with 0.4 DS was selected as an example for scaffold preparation as the higher degree of substitution polymer tend to lose its solubility in water and lower degree of substitution fails to provide adequate mechanical properties. Aqueous HPC exhibits low critical solution temperature

(LCST) transition, from isotropic solutions at room temperature to metastable colloidal systems upon heating.[24,26] This thermal-induced phase separation is due to dehydration of HPC and consequently increased hydrophobic associations among HPC molecules with increasing temperature. HPC-MA retains the phase behavior characteristic of HPC, as demonstrated in the turbidity measurement shown in Figure 1 ($p < 0.05$, $n = 4$). The first sign of turbidity was observed at approximately 36 °C. The LCST of HPC-MA was determined to be approximately 37 to 38 °C, after which the transmittance decreases drastically with increasing temperature until reaching a plateau at ~45 °C.

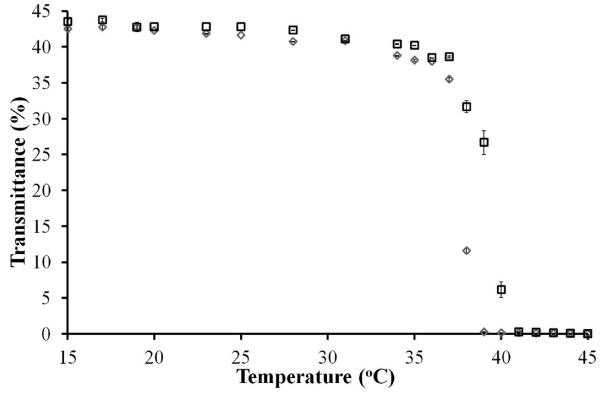

Figure 1. Turbidimetry measurement for HPC-MA-15% (black □) and HPC-MA-20% (gray ◇).The percent transmittance decreases as the temperature increases ($p < 0.05$, $n = 4$). Data are shown as mean values with standard deviation as error bars in the form of mean value ± standard deviation.

Physiochemical Characterization of HPC-MA Hydrogels. UV-irradiation was selected to induce cross-linking of aqueous HPC-MA due to its many advantages, including fast polymerization rate at low temperature and ease of hydrogel shaping.[34] The photoinitiator, 2-hydroxy-1-[4-(2-hydroxyethoxy)phenyl]-2-methyl-1-propanone (Irgacure 2959), has shown to cause minimal toxicity to a wide range of mammalian cells[35] and, therefore, was employed for the preparation of HPC-MA-15% and HPC-MA-20% hydrogel samples. Figure 2 shows the representative photos of the water contact angles on HPC-MA-20% at 25, 37, and 42 °C, as the testing temperature is increased from 25 to 37 °C; the water contact angle of the HPC-MA gel increased from 35.1° to 52.1°, reflecting an increase in surface hydrophobicity. This finding revealed that the thermoresponsive behavior of HPC-MA conjugates was retained after cross-linking, resulting in chemically cross-linked thermoresponsive hydrogels that underwent phase transition at an onset temperature of 37 °C. A further increased in temperature above the HPC-MA gel LCST results in a contact angle of 61°.

Equilibrium swelling of HPC-MA hydrogels was measured gravimetrically at 4, 25, 37, and 42 °C. Figure 3 shows that as the temperature increases, the equilibrium swelling ratio decreases ($p < 0.05$, $n = 5$), indicating that the hydrogels undergo a temperature-triggered deswelling process. The magnitude of change in equilibrium swelling ratio of the hydrogels, from a swollen to deswollen state, decreases as the polymer concentration in the hydrogels increases from 15% to 20% (w/v). Concurrently, the hydrogels also change their appearances from transparent to opaque as the temperatures rises above 42 °C (Figure 4).

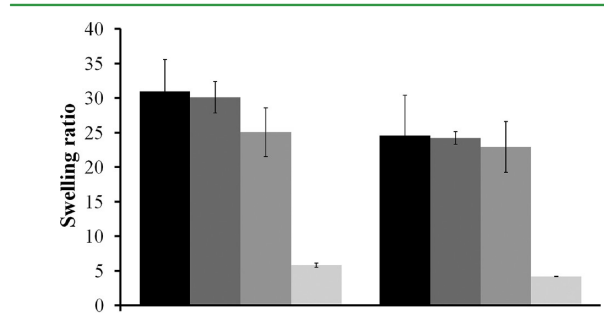

Figure 3. Swelling ratio for HPC-MA-15% and HPC-MA-20% at 4 °C (black bar), 25 °C (dark gray bar), 37 °C (medium gray bar), and 42 °C (light gray bar). The swelling ratio decreases as the temperature increases ($p < 0.05$, $n = 5$). Data are shown as mean values with standard deviation as error bars in the form of mean value ± standard deviation.

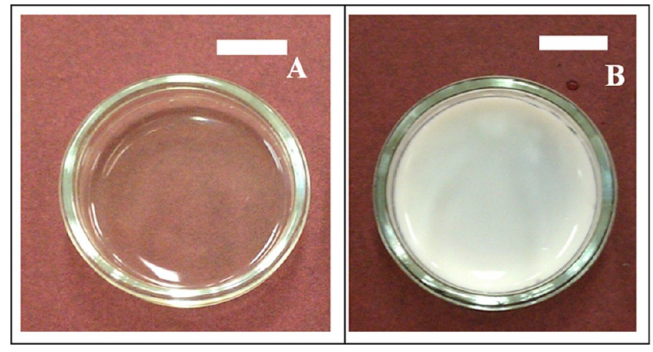

Figure 4. Thermal sensitivity of HPC-MA gel (scale bar of 1 cm) at 25 °C (A) and 42 °C (B).

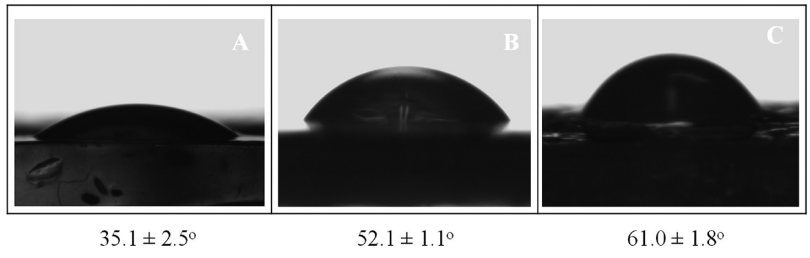

Figure 2. Contact angle of HPC-MA-20% gel at room temperature (A), 37 °C (B), and 42 °C (C). Data are shown as mean values with standard deviation as error bars in the form of mean value ± standard deviation.

HPC-MA contains both hydrophilic and hydrophobic groups. At temperature below the lower critical solution temperature, the hydrophilic groups of the HPC-MA in the hydrogels bond to water molecules through hydrogen bonds to form a stable shell around the hydrophobic groups, hence giving rise to a high equilibrium swelling ratio and low water contact angle. As seen from Figure 3, the equilibrium swelling ratio starts to decrease at approximately 37 °C. This is due to breaking of the hydrogen bonds between the water molecules and/surrounding the polymer at elevated temperature, and consequently the interactions among the hydrophobic groups become dominant. As a result, the water molecules are released out, and the polymer networks in the hydrogels collapse with increased hydrophobicity, similar behavior has been observed for other types of thermo-responsive hydrogel systems.[36,37]

Storage moduli of HPC-MA-15% and HPC-MA-20% are shown in Figure 5 as a function of temperature. It is well-known that cross-linking density in hydrogel increases with increasing polymer concentration due to the formation of longer attached chain,[4,38] and a densely cross-linked network exhibits higher mechanical strength compared to loosely cross-linked network. As expected, the storage modulus of the hydrogels increases with increasing the polymer concentration from 15% to 20% (w/v). As temperature increases from 25 to 45 °C, the storage modulus increases from 0.7 to 0.9 kPa for HPC-MA-15%, and from 1.9 to 2.5 kPa from HPC-MA-20%, respectively. The HPC-MA hydrogels exhibit temperature dependent storage modulus; a similar trend has also been reported for other types of thermoresponsive hydrogels, such as a hydrogel composed of PNIPAAm and methylcellulose.[39] As the temperature rises above the LCST, the polymer chains within hydrogel undergo coil−globule transition, leading to a more densely packed network, thereby exhibiting higher storage modulus. The mechanical property of a hydrogel is an important factor for promoting tissue repair and regeneration.[40,41] Different targeted tissue types require the use of hydrogels with matching mechanical properties for cell cultivation. The range of storage modulus exhibited by the HPC-MA hydrogels is comparable to that of soft tissues and organs such as brain, lymph node, mammary gland, liver, breast tumor, and kidney,[42] which suggests that they can be used as biomimicry culture substrates to simulate these soft tissues. Further fine-tuning of the mechanical properties of HPC-MA hydrogels can be achieved by varying the concentration and degree of substitution of HPC-MA.

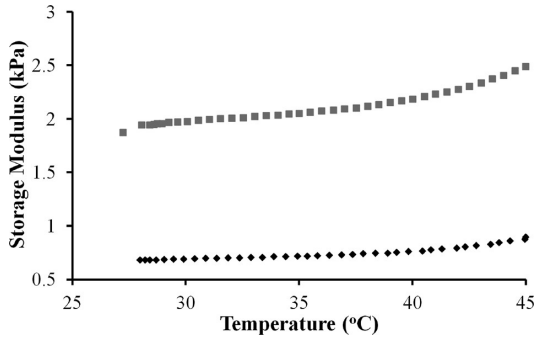

Figure 5. Storage modulus for HPC-MA-15% (black ◆) and HPC-MA-20% (gray ■).

Cell Proliferation on HPC-MA Hydrogels. To assess the cytocompatibility of the HPC-MA hydrogels, COS-7 cells were seeded onto the surface of HPC-MA-20% hydrogel as shown in Figure 6A and cultured at 37 °C in a humidified 5% CO_2 incubator. Figure 6B−E shows that COS-7 cells exhibited spindle morphology and reached confluency after 5 days, indicating that these cells adhered well on the hydrogel. The number of cells proliferated on the hydrogel was quantified by determining the DNA content, because DNA is the cellular component that reflects the cell number most accurately.[43] Figure 7 shows that the DNA content, and hence the number of cells, on the hydrogel increased over the 5 day period ($p < 0.05$, $n = 4$), indicating that the HPC-MA hydrogel is biocompatible to COS-7 cells and facilitate cell proliferation.

Temperature-Dependent Cell-Release Behavior. Traditionally, to detach cells that adhere to culture surfaces, enzymatic digestion such as trypsin or Dispase is utilized. Such

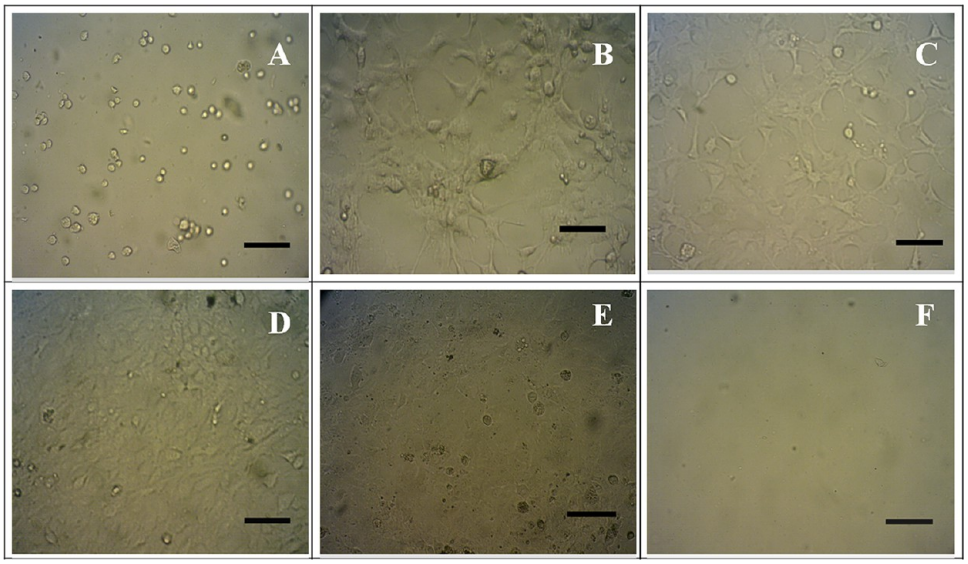

Figure 6. COS 7 cell growth (scale bar of 100 μm): day 0 (A), day 2 (B), day 3 (C), day 4 (D), day 5 (E) on hydrogel, and the surface of hydrogel after cold treatment (F).

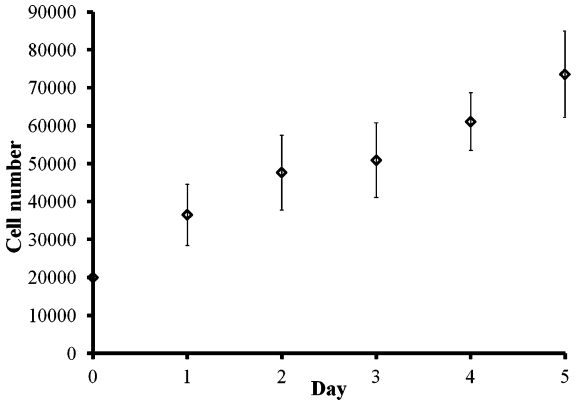

Figure 7. Proliferation of COS-7 cells on HPC-MA-20% hydrogel. Cell growth on hydrogel increased gradually over a period of 5 days ($p < 0.05$, $n = 4$). Data are shown as mean values with standard deviation as error bars in the form of mean value ± standard deviation.

detachment of cells caused the destruction of extracellular matrix, growth factor receptors, and cellular junctions.[1,5,6] In this study, COS-7 cells are employed for monitoring cell attachment on and detachment from the HPC-MA hydrogel surfaces, because of their rapid division and growth.[44] Cells were seeded onto the surface of HPC-MA-20% hydrogel. At day 4, the hydrogel was subjected to cold treatment at 4 °C for 30 min. It was found that approximately 80 to 90% of the attached cells were detached from the hydrogel by this cold treatment (Figure 6F). At the onset LCST, cells adhere on the hydrogel surface passively due to hydrophobic interaction between the cells and the gel surface. During cold treatment, the hydrogel undergoes phase transition and becomes hydrophilic which is less favorable to cell adhesion, thus causing the cells to detach from the hydrogel surface. The detachment of cells is accelerated probably due to water penetration as the hydrogel underwent low temperature induced swelling. In another set of experiment, COS-7 cells were allowed to cultivate for 10 day (Figure 8A) followed by cold treatment.

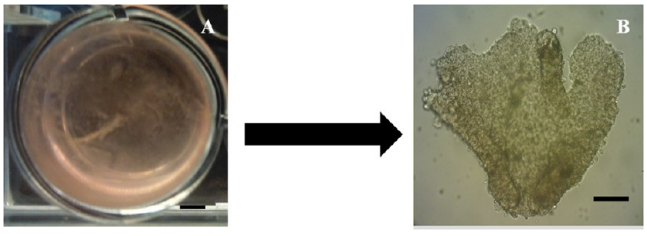

Figure 8. (A) COS 7 cells grown on hydrogel (scale bar 0.2 cm) at day 10. The hydrogel was subjected to cold treatment; the cell sheet was then transferred to a culture dish. (B) Representative image showing a cell sheet retrieved after cold treatment (scale bar 100 μm).

Figure 8B shows that a detached COS-7 cell sheet was transferred and readhered on a culture dish after cold treatment without trypsin treatment. It was observed that cell−cell connections were maintained after cold detachment, which is important for tissue regeneration.

Similar process involving cell seeding, attachment and detachment was carried out using Oct4b2 cells. Figure 9A−D shows the cells seeded on hydrogel at day 0 and cell growth on hydrogel at day 3. At day 3, the cultured Oct4b2 cells were detached from the hydrogel followed by incubation at 4 °C for 10 min. Reculturing of the detached Oct4b2 cells onto a new

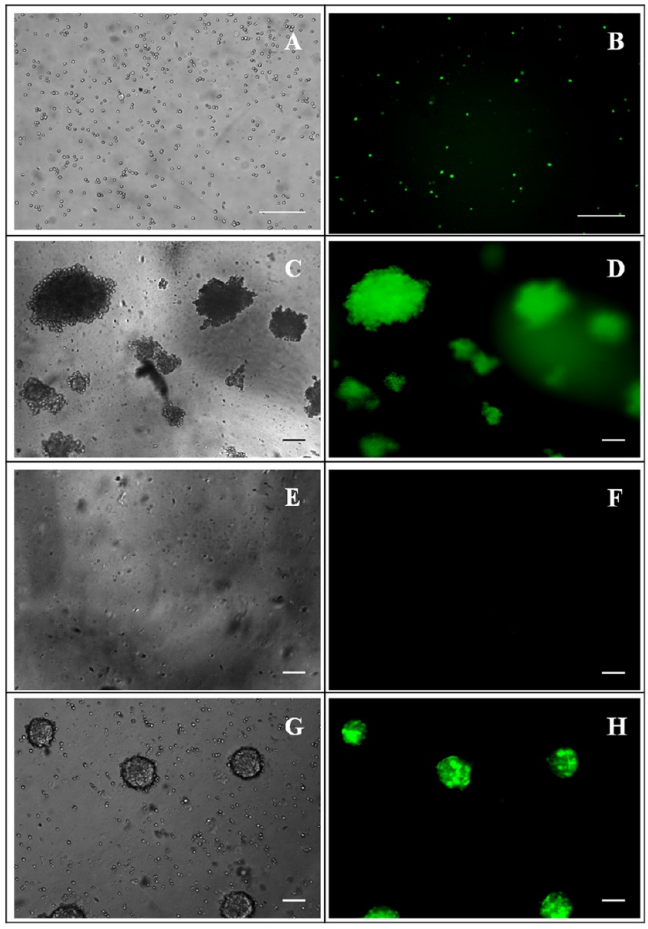

Figure 9. Representative images showing bright field and GFP expression of Oct4b2 cells growth (scale bar of 100 μm) at day 0 (A, B), and day 3 on hydrogel (C, D). Oct4b2 cells were cultured on a hydrogel for a period of 3 days, the hydrogel was then subjected to cold treatment, and the detached cells were transfer to a culture dish for readhesion. Representative images show the (E) bright field and (F) GFP filter view of the surface of hydrogel after cold treatment; apart from debris, very little cells and GFP signal can be detected, indicating that the cold treatment can detach most of the cells from the hydrogel. Representative images show the (G) bright field and (H) GFP filter view of cells retrieved after cold treatment; images were taken on day 3 after the retrieved cells were transferred to a culture dish.

tissue-culture plate was undertaken to preliminarily access the viability of the detached cells. Oct4b2 cells carry the Oct4-green fluorescence protein (Oct4-GFP) reporter, and the Oct4-GFP expression is directly correlated with the pluripotency of these cells. During the course of the experiment, the GFP expression of Oct4b2 cells was monitored using a fluorescence microscope. Figure 9E and F shows that the detached Oct4b2 cells demonstrated good viability and healthy morphology of the Oct4b2 cells as compared to Oct4b2 cells cultured on T-flask without cold treatment (control) in Figure 10. The Oct4-GFP expression observed in Oct4b2 cells at day 3 in Figure 9G and H revealed that the pluripotency of Oct4b2 cells were maintained after the cold treatment of the hydrogel, indicating that these cells can be further proliferated for tissue engineering applications.

Cell Viability after Cold Treatment. COS-7 cells were cultured on the hydrogel as described above. At day 4, the hydrogel was subjected to cold treatment at 4 °C for 30 min.

dx.doi.org/10.1021/am4009133 | ACS Appl. Mater. Interfaces 2013, 5, 5592−5600

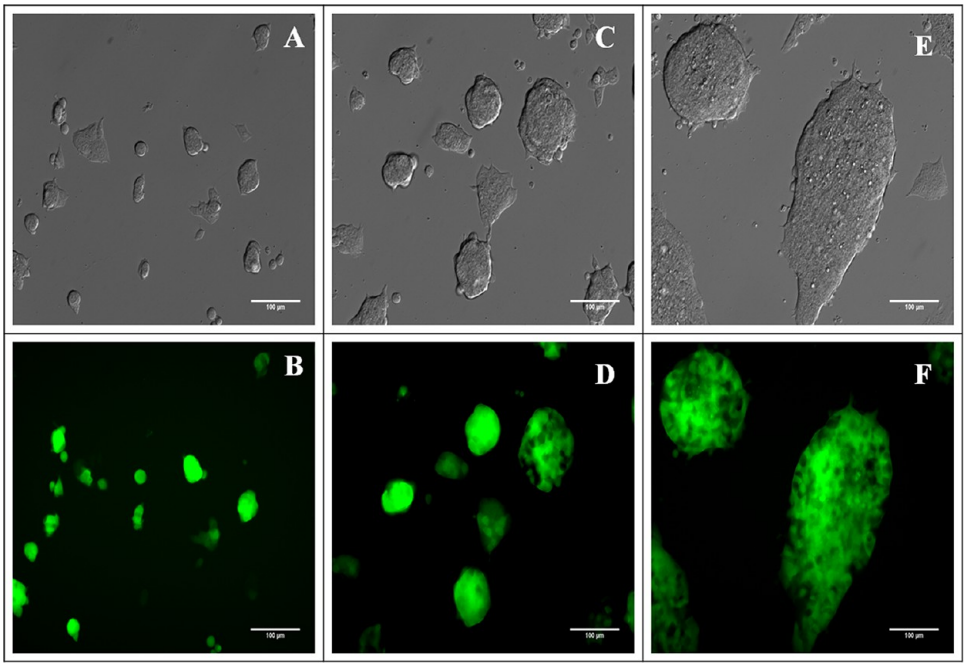

Figure 10. Bright field and GFP expression of Oct4b2 cells growth on culture dish (scale bar of 100 μm): day 1 (A, B), day 2 (C, D), and day 3 (E, F).

The readhesion and proliferation of the detached COS-7 cells were assessed preliminarily by reculturing them onto a well-plate and measured using alamarBlue assay. Figure 11A shows a

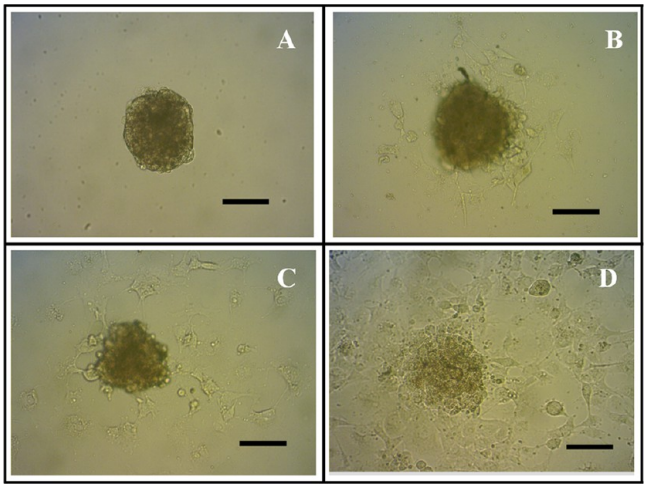

Figure 11. COS 7 cells were cultured on hydrogel for 4 days followed by cold treatment. The detached cells were allowed to readhere and proliferate on culture dish for (a) 0 day, (B) 1 day, (C) 3 days, and (D) 4 days (scale bar of 100 μm).

photo of the detached cell sheet from the hydrogel after cold treatment. The harvested cell sheet shrunk due to the inherent contractile force within cells and their connectivity to the sheet, similar phenomena was observed by other study that retrieve cell sheet from poly(NIPAAm) substrate.[45] Hirose et al.[46] demonstrated that the use of a hydrophilically modified polyvinylidenefluoride membrane as a supporter can prevent the cell sheet from shrinkage and wrinkling when transferring the cell sheet to another surface, such support membrane can be used in future study to prevent the shrinkage of the harvested cell sheet. Nevertheless, once the cell sheet from HPC-MA hydrogel was allowed to readhere on a culture dish, the cell sheet started to spread out as the cells started to adhere and migrate along the culture dish (Figure 11B–D). It was shown that these cells adhered well to the new surface and resumed normal growth (Figures 11 and 12). Figure 12 shows

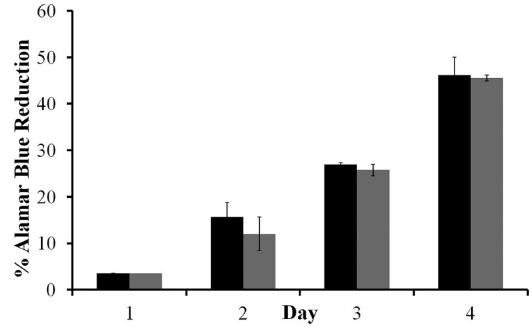

Figure 12. Cell viability of COS-7 cells with cold treatment (gray bar) compared to cells without hydrogel and cold treatment (black bar) (control) in terms of percent reduction in alamarBlue. No significant difference in viability of cold treated cells and control cells was observed ($p < 0.05$, $n = 3$). Data are shown as mean values with standard deviation as error bars in the form of mean value ± standard deviation.

the viability of cells after undergoing cold treatment as compared to cells that have not been cultured on hydrogel and have not been subjected to cold treatment (control). The metabolic activity of cells causes a chemical reduction of the alamarBlue reagent and leads to color change in this redox indicator. In another word, the increase in metabolic activity increases the amount of reduced alamarBlue.[47] The result shows that there is no significant difference in percentage of alamarBlue reduction in both the cold treated cells and control cells ($p < 0.05$, $n = 3$). The increase in percentage of alamarBlue reduction from ~3.5% to ~46% indicates that the cells are not

dx.doi.org/10.1021/am4009133 | ACS Appl. Mater. Interfaces 2013, 5, 5592–5600

only viable but also proliferate continuously, thus revealing that the cells were not affected by undergoing cold treatment as compared to control cells. This indicates that the cells retrieved from the hydrogel can be further proliferated for tissue engineering applications. After cold treatment, the number of cells was quantified by measuring the DNA content. Figure 13

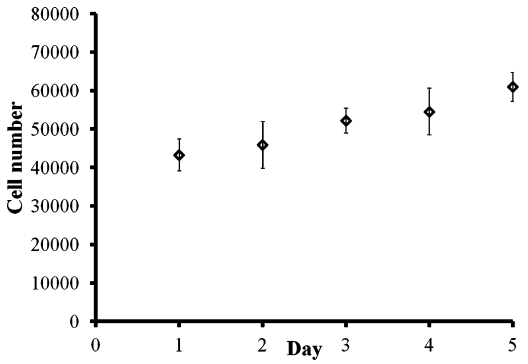

Figure 13. Proliferation of COS-7 cells that were harvested from hydrogel using cold treatment. COS 7 cells were firsts cultured on hydrogel for 4 days followed by cold treatment; the detached cells were allowed to readhere and proliferate on culture dish. The number of cells increased gradually over a period of 5 days ($p < 0.05$, $n = 6$). The data are shown as mean values with standard deviation as error bars in the form of mean value ± standard deviation.

shows that the cell number increases over a period of 5 days ($p < 0.05$, $n = 6$). The growth of cold-treated cells was observed to be slower compared to those grew on hydrogel before cold treatment. This is probably due to uneven cell seeding, as the cold-treated cells were readhered on a culture plate as cell sheet without further trypsinization, the proliferation of cells at the center of a cell sheet is restricted due to the lack of space. As shown in Figure 11, those cells at the center of the cell sheet need to migrate out first before proceeding to proliferation. Nonetheless, the increase in cell number confirmed that cells retained their proliferation ability after cold treatment.

The findings from this study suggest that the HPC-MA hydrogel possess thermoresponsive properties and exhibit temperature dependent cell-release behavior. It is worthwhile to mention that the LCST of HPC-MA can be further modulated by engineering the side chain chemistry. The influence of introduced side groups on the thermal-responsive properties of HPC-MA hydrogel is currently under investigation.

CONCLUSION

Serving as a proof of concept study, thermoresponsive cellulosic hydrogels were prepared by UV cross-linking aqueous HPC-MA at room temperature. The hydrogels exhibit temperature-modulated characteristics including surface hydrophilicity and hydrophobicity, equilibrium swelling and deswelling, as well as mechanical properties. A LCST of HPC-MA conjugate was found to be ∼37−38 °C as determined by turbidity measurement. Cell-releasing characteristics were demonstrated using COS-7 cells and Oct4b2 cells. Both COS-7 and Oct4b2 cells adhere and proliferate well on the hydrogel surfaces under normal cell-culture conditions. By reducing the temperature to 4 °C, the cultivated cells spontaneously detach from the hydrogels without trypsin treatment. These unique properties of HPC-MA hydrogels would make them potential culture substrates for cell sheet engineering.

AUTHOR INFORMATION

Corresponding Author

* (P.P.Y.C.) Tel: +613 9925 2660. E-mail: peggy.chan@rmit.edu.au. (Z.Y.) Tel: +612 4221 3832. E-mail: zyue@uow.edu.au.

Notes

The authors declare no competing financial interest.

ACKNOWLEDGMENTS

Funding for this research was partly provided through an Australia Research Council Discovery Project Grant ARC DP 120102570. We also thank Dr. Paul Verma from Monash Institute of Medical Research (MIMR) for supplying Oct4b2 cells. We would like to thank Prof. Robert Shanks and Izan Roshawaty Mustapa for their assistance with DMA measurements. This work was performed in part at the Melbourne Centre for Nanofabrication, an initiative partly funded by the Commonwealth of Australia and the Victoria Government. P.P.Y.C. is grateful for a MCN Technology Fellowship and a RMIT University Senior Research Fellowship that supported this work.

REFERENCES

(1) Shimizu, T.; Yamato, M.; Kikuchi, A.; Okano, T. *Biomaterials* **2003**, *24* (13), 2309−2316.
(2) Iwata, T.; Yamato, M.; Okano, T. Intelligent Surfaces for Cell-Sheet Engineering. In *Principles of Regenerative Medicine*, second ed.; Atala, A., Lanza, R., Thomson, J., Nerem, R., Eds.; Academic Press: San Diego, 2011; Chapter 29, pp 517−527.
(3) Zahn, R.; Thomasson, E.; Guillaume-Gentil, O.; Voros, J.; Zambelli, T. *Biomater* **2012**, *33* (12), 3421−7.
(4) Lee, F.; Chung, J. E.; Kurisawa, M. *J. Controlled Release* **2009**, *134* (3), 186−193.
(5) Biazar, E.; Montazeri, N.; Pourshamsian, K.; Asadifard, F.; Ghorbanalinezhad, E.; Keshel, S. H.; Hashemi, M.; F.H, S. R.; Majdi, A. *J. Paramed. Sci.* **2010**, *1* (3), 27−33.
(6) Yamato, M.; Akiyama, Y.; Kobayashi, J.; Yang, J.; Kikuchi, A.; Okano, T. *Prog. Polym. Sci.* **2007**, *32* (8−9), 1123−1133.
(7) da Silva, R. M. P.; Mano, J. F.; Reis, R. L. *Trends Biotechnol.* **2007**, *25* (12), 577−583.
(8) Wu, J.-Y.; Liu, S.-Q.; Heng, P. W.-S.; Yang, Y.-Y. *J. Controlled Release* **2005**, *102* (2), 361−372.
(9) Okano, T. *Rinsho Shinkeigaku* **2006**, *46* (11), 795−798.
(10) Biazar, E.; Pourshamsian, K. *Orient. J. Chem.* **2011**, *27* (4), 1443−1449.
(11) Haraguchi, Y.; Shimizu, T.; Yamato, M.; Okano, T. *Cardiol. Res. Practice* **2011**, *2011*, 1−8.
(12) Masuda, S.; Shimizu, T.; Yamato, M.; Okano, T. *Adv. Drug Delivery Rev.* **2008**, *60* (2), 277−285.
(13) Sakaguchi, K.; Shimizu, T.; Horaguchi, S.; Sekine, H.; Yamato, M.; Umezu, M.; Okano, T. *Sci. Rep.* **2013**, *3*, 1316.
(14) Wang, T.; Liu, D.; Lian, C.; Zheng, S.; Liu, X.; Wang, C.; Tong, Z. *React. Funct. Polym.* **2011**, *71* (4), 447−454.
(15) Vihola, H.; Laukkanen, A.; Valtola, L.; Tenhu, H.; Hirvonen, J. *Biomater* **2005**, *26* (16), 3055−3064.
(16) Chen, B.; Dang, J.; Tan, T. L.; Fang, N.; Chen, W. N.; Leong, K. W.; Chan, V. *Biomater* **2007**, *28* (8), 1503−1514.
(17) Haraguchi, K.; Takehisa, T.; Ebato, M. *Biomacromolecules* **2006**, *7* (11), 3267−3275.
(18) Chen, C.-H.; Tsai, C.-C.; Chen, W.; Mi, F.-L.; Liang, H.-F.; Chen, S.-C.; Sung, H.-W. *Biomacromolecules* **2006**, *7* (3), 736−743.
(19) Kim, Y. S.; Lim, J. Y.; Donahue, H. J.; Lowe, T. L. *Tissue Eng* **2005**, *11* (1−2), 30−40.

(20) Zhang, H.; Iwama, M.; Akaike, T.; Urry, D. W.; Pattanaik, A.; Parker, T. M.; Konishi, I.; Nikaido, T. *Tissue Eng.* **2006**, *12* (2), 391−401.
(21) Guillaume-Gentil, O.; Akiyama, Y.; Schuler, M.; Tang, C.; Textor, M.; Yamato, M.; Okano, T.; Vörös, J. *Adv. Mater.* **2008**, *20* (3), 560−565.
(22) Edahiro, J.-i.; Sumaru, K.; Tada, Y.; Ohi, K.; Takagi, T.; Kameda, M.; Shinbo, T.; Kanamori, T.; Yoshimi, Y. *Biomacromolecules* **2005**, *6* (2), 970−974.
(23) Nagai, N.; Yunoki, S.; Satoh, Y.; Tajima, K.; Munekata, M. *J. Biosci. Bioeng.* **2004**, *98* (6), 493−496.
(24) Yue, Z.; Wen, F.; Gao, S.; Ang, M. Y.; Pallathadka, P. K.; Liu, L.; Yu, H. *Biomaterials* **2010**, *31* (32), 8141−521.
(25) Hussain, M. A. *J. Polym. Sci., Part A: Polym. Chem.* **2008**, *46* (2), 747−752.
(26) Hirsch, S. G.; Spontak, R. J. *Polymer* **2002**, *43* (1), 123−129.
(27) Francis, M. F.; Piredda, M.; Winnik, F. M. *J. Controlled Release* **2003**, *93* (1), 59−68.
(28) Hoo, S. P.; Loh, Q. L.; Yue, Z.; Fu, J.; Tan, T. T. Y.; Choong, C.; Chan, P. P. Y. *J. Mater. Chem. B* **2013**, *1* (24), 3107−3117.
(29) Yeom, Y. I.; Fuhrmann, G.; Ovitt, C. E.; Brehm, A.; Ohbo, K.; Gross, M.; Hubner, K.; Scholer, H. R. *Development* **1996**, *122* (3), 881−894.
(30) Sarvi, F.; Yue, Z.; Hourigan, K.; Thompson, M. C.; Chan, P. P. Y. *J. Mater. Chem. B* **2013**, *1* (7), 987−996.
(31) Yue, Z.; Cowie, J. M. G. *Polymer* **2002**, *43* (16), 4453−4460.
(32) Zhang, Z. B.; McCormick, C. L. *J. Appl. Polym. Sci.* **1997**, *66* (2), 293−305.
(33) Montalbetti, C. A. G. N.; Falque, V. *Tetrahedron* **2005**, *61* (46), 10827−10852.
(34) Benson, R. S. *Nucl. Instrum. Methods Phys. Res., Sect. B* **2002**, *191* (1−4), 752−757.
(35) Nair, L. S.; Laurencin, C. T.; Tandon, M. Injectable Hydrogels as Biomaterials. In *Advanced Biomaterials*; Basu, B., Kati, D. S., Kumar, K., Eds.; John Wiley & Sons, Inc.: Hoboken, NJ, 2010; pp 179−203.
(36) Cole, M. A.; Voelcker, N. H.; Thissen, H.; Griesser, H. J. *Biomaterials* **2009**, *30* (9), 1827−1850.
(37) Temtem, M.; Casimiro, T.; Mano, J. F.; Aguiar-Ricardo, A. *Green Chem.* **2007**, *9* (1), 75−79.
(38) Wang, L. S.; Chow, P. Y.; Phan, T. T.; Lim, I. J.; Yang, Y. Y. *Adv. Funct. Mater.* **2006**, *16* (9), 1171−1178.
(39) Liu, W.; Zhang, B.; Lu, W. W.; Li, X.; Zhu, D.; De Yao, K.; Wang, Q.; Zhao, C.; Wang, C. *Biomaterials* **2004**, *25* (15), 3005−3012.
(40) Nicodemus, G. D.; Bryant, S. J. *Tissue Eng., Part B* **2008**, *14* (2), 149−65.
(41) Straley, K. S.; Foo, C. W.; Heilshorn, S. C. *J. Neurotrauma* **2010**, *27* (1), 1−19.
(42) Levental, I.; Georges, P. C.; Janmey, P. A. *Soft Matter* **2007**, *3* (3), 299−306.
(43) Rage, R.; Mitchen, J.; Wilding, G. *Anal. Biochem.* **1990**, *191* (1), 31−34.
(44) Knapek, K.; Frondorf, K.; Post, J.; Short, S.; Cox, D.; Gomez-Cambronero, J. *Mol. Cell. Biol.* **2010**, *30* (18), 4492−506.
(45) Mizutani, A.; Kikuchi, A.; Yamato, M.; Kanazawa, H.; Okano, T. *Biomaterials* **2008**, *29* (13), 2073−2081.
(46) Hirose, M.; Kwon, O. H.; Yamato, M.; Kikuchi, A.; Okano, T. *Biomacromolecules* **2000**, *1* (3), 377−381.
(47) Das, G. K.; Chan, P. P. Y.; Teo, A.; Loo, J. S. C.; Anderson, J. M.; Tan, T. T. Y. *J. Biomed. Mater. Res., Part A* **2010**, *93A* (1), 337−346.
(48) Kushida, A.; Yamato, M.; Konno, C.; Kikuchi, A.; Sakurai, Y.; Okano, T. *J. Biomed. Mater. Res.* **2000**, *51* (2), 216−223.